ISSN 0915-633X

INTERNATIONAL ATOMIC ENERGY AGENCY

FIFTEENTH INTERNATIONAL CONFERENCE ON PLASMA PHYSICS AND CONTROLLED NUCLEAR FUSION RESEARCH

Seville, Spain, 26 September – 1 October 1994

IAEA-CN-60/D-P-I-14

NATIONAL INSTITUTE FOR FUSION SCIENCE

Monte Carlo Simulation for ICRF Heating in Heliotron/Torsatrons

S. Murakami, M. Okamoto, N. Nakajima, K.Y. Watanabe,
T. Watari, T. Mutoh, R. Kumazawa and T. Seki

(Received - Aug. 26, 1994)

NIFS-306 Sep. 1994

This report was prepared as a preprint of work performed as a collaboration research of the National Institute for Fusion Science (NIFS) of Japan. This document is intended for information only and for future publication in a journal after some rearrangements of its contents.

Inquiries about copyright and reproduction should be addressed to the Research Information Center, National Institute for Fusion Science, Nagoya 464-01, Japan.

RESEARCH REPORT
NIFS Series

This is a preprint of a paper intended for presentation at a scientific meeting. Because of the provisional nature of its content and since changes of substance or detail may have to be made before publication, the preprint is made available on the understanding that it will not be cited in the literature or in any way be reproduced in its present form. The views expressed and the statements made remain the responsibility of the named author(s); the views do not necessarily reflect those of the government of the designating Member State(s) or of the designating organization(s). *In particular, neither the IAEA nor any other organization or body sponsoring this meeting can be held responsible for any material reproduced in this preprint.*

NAGOYA, JAPAN

INTERNATIONAL ATOMIC ENERGY AGENCY

FIFTEENTH INTERNATIONAL CONFERENCE ON PLASMA PHYSICS AND CONTROLLED NUCLEAR FUSION RESEARCH

Seville, Spain, 26 September – 1 October 1994

IAEA-CN-60/D-P-I-14

MONTE CARLO SIMULATION FOR ICRF HEATING IN HELIOTRON/TORSATRONS

S. MURAKAMI, M. OKAMOTO, N. NAKAJIMA, K. Y. WATANABE,

T. WATARI, T. MUTOH, R. KUMAZAWA, and T. SEKI

National Institute for Fusion Science, Nagoya 464-01, Japan

Keywords : Monte Carlo simulation, ICRF minority heating, Large Helical Device, heating efficiency, finite beta effects, orbit loss, radial electric field

This is a preprint of a paper intended for presentation at a scientific meeting. Because of the provisional nature of its content and since changes of substance or detail may have to be made before publication, the preprint is made available on the understanding that it will not be cited in the literature or in any way be reproduced in its present form. The views expressed and the statements made remain the responsibility of the named author(s); the views do not necessarily reflect those of the government of the designating Member State(s) or of the designating organization(s). *In particular, neither the IAEA nor any other organization or body sponsoring this meeting can be held responsible for any material reproduced in this preprint.*

ABSTRACT

A Monte Carlo simulation code has been developed for studying ICRF minority heating in heliotron/torsatrons, which includes complicated orbits of high energetic particles, Coulomb collisions, interactions between the particles and the applied RF-field, and the self-determined radial electric field in the finite β equilibrium. Calculations have been carried out using the code to study physics of ICRF minority heating in heliotron/torsatrons taking the Large Helical Device as an example. The radial electric field is self-consistently determined taking into account orbit loss of accelerated minority ions. Common characteristics of physics of ICRF minority heating in heliotron/torsatrons, such as effects of finite β, location of resonance layer, finite $k_{||}$, localization of the RF-field, minority species, and the radial electric field, are clarified.

1. INTRODUCTION

Experiments of ICRF heating have been carried out (Heliotron-E[1,2], ATF[3], and CHS[4]) and the possibility of this heating method in heliotron/torsatrons has been demonstrated. We expect that the ICRF heating will be a powerful means to heat the plasma of the Large Helical Device (LHD) [5]. We are developing ICRF heating antennas for the LHD with output power of 12MW (10 seconds) and 3MW (steady state). The frequency f can be varied from 25MHz to 95MHz to realize a variety of ICRF heatings. We install the antennas for fast-wave heating near the helical coil on the larger major radius side where the plasma cross sections are vertically elliptic. The two ion-hybrid resonance is located in the central region of the plasma when f = 45MHz and B = 3T, and direct electron heating can be possible through mode conversion. Minority heating (H or ^{3}He) is also possible when the minority concentration is small. If the frequency is raised, only ion heating takes place in a similar way to low-field-side launching in tokamaks. For f = 54MHz and B = 3T, the resonance surface is located only on the inside of the torus and trapped particles heated by the RF-wave would be localized and less particle orbit loss may be expected.

In heliotron/torsatrons, the magnetic field configurations are so complicated that the orbits of high energetic particles deviate largely from the magnetic flux surface. The field configuration becomes more complicated as the plasma β value increases to enhance loss of trapped particles. Accordingly, it is necessary to perform an orbit following/Monte Carlo simulation to take into account orbit effects correctly in studying ICRF heating.

In this paper we study physics of ICRF heating of the plasma in heliotron/torsatrons taking the LHD as an example using the Monte Carlo simulation code, MOMOCO, in which finite β effects, complicated orbits of high energy particles, Coulomb collisions, interactions between the particles and the RF-field, and the self-determined radial electric field, are included[6,7]. The effects of the finite $k_{||}$ and $k_{\perp}$ are also included in this study.

The LHD is a helical system with L = 2 and M = 10 heliotron/torsatron configuration, where R = 3.9m, $\bar{a}_p$ = 0.55 ~ 0.65m, α = 0.1 (α : the pitch modulation parameter of the winding law), and γ_c = 1.25 (γ_c: the pitch parameter). We, here, use the LHD configuration called "the standard configuration", in which the shift of the vacuum magnetic axis position, Δ, is −0.15m (0.15m inward shift) and the toroidally averaged magnetic surfaces are nearly circular in the vacuum field. This configuration satisfies the requirements for high plasma performance, i.e. a good bulk particle confinement, a high plasma β, and creating a divertor configuration.

Using the vacuum magnetic field configuration, we solve the three dimensional finite β MHD equilibrium by the VMEC code[8] under the fixed boundary condition and $P = P_0(1 - \psi/\psi_a)^2$. And we study the effects of the finite β on the ICRF minority heating based on the obtained MHD equilibrium.

Effects of the radial electric field is also studied. In helical systems the radial electric field, E_ψ, much affects particle motions not only at the plasma periphery but also near the center of plasma[9,10]. Some of trapped high energetic minority ions accelerated by the RF-field may escape out of the last closed magnetic surface, making the large particle flux in the radial direction. This must contribute to create the radial electric field together with majority ions and electrons. The radial electric field will be determined self-consistently including escaping energetic minority ions.

2. EFFICIENCIES OF ICRF MINORITY HEATING

We perform a large number of simulation runs changing the plasma β, the strength of wave electric field, E_{RF}, and the position of resonance layer.

The velocity and pitch angle of minority ion are changed due to the interaction with the RF-wave and the transition of particle motions from untrapped to trapped or from trapped to untrapped occurs. Figure 1 shows typical trajectories of a selected minority ion during the calculations including collisions and interactions with the RF-wave for two different β values; (a) β_0 = 0.0% and (b) β_0 = 6.0. The radial electric field is not contained. The transition of the particle motion due to the RF wave can be seen. Additionally in the case of β_0 = 6.0 the loss of the minority ion is found because of the configuration changes due to the finite beta effects.

We next show the finite β effect on the heating efficiency of the ICRF minority heating. We define the heating efficiency by P_{trans}/P_{abs} where P_{trans} and P_{abs} are the transferred power from the minority ions to the background plasma and the absorbed power from the RF wave to the minority ions, respectively. We set Z_{eff} = 1.0 and the parameters at the plasma center as $n_0 = 1.0 \times 10^{20}\mathrm{m}^{-3}$, T_{e0} = 1.0keV, and T_{i0} = 1.0keV. And we assume the H or ^{3}He minority ion and 3% of the minority ion fraction. Figure 2 shows the plots of heating efficiency versus P_{abs}. The strengths of the resonance magnetic field are set to the value at the magnetic axis. The absorption power is changed by changing the RF electric field on the resonance layer from $E_{RF} = 1.0 \times 10^3$V/m to $E_{RF} = 3.0 \times 10^3$V/m in this Figure. In the case of β_0 = 0.0% (H minority), the heating efficiency is 92% for P_{abs} = 2MW and decreases monotonically with increasing in P_{abs}. For finite β values (β_0 = 4.0 and 6.0%) the heating efficiencies are around 70% when $P_{abs} \leq$ 5MW. However, no remarkable differences in heating efficiencies are found for different β values (β_0 = 0.0, 4.0, 6.0%) in the region of high absorption power (P_{abs} > 5MW). It is found that the heating efficiencies for ^{3}He minority cases (open circles, triangles, squares) are up to 30% higher than those of H minority cases. And the large increase in the transferred power to majority ions is found in the ^{3}He minority case.

The radial profile of the transferred power from accelerated minority ions to majority ions and electrons, or deposition profile, is different for a finite β plasma from that of a vacuum plasma. In the case of β_0 = 0, the deposition profile has a peak near the center and decreases roughly monotonically with the plasma radius. On the other hand the second peak appears near the plasma periphery as well as near the center in the case of β_0 = 6%. This fact shows that the deposition profile changes for the finite β plasma is attributed to the topological change of the trapped particles. Deeply trapped particles (contour of mod-B_{min}) has a bean-shaped trajectory because of the finite β effect.

The influence of the position of resonance layer on the heating efficiency is also studied changing the applied wave frequency. In the case of β_0 = 0.0% the heating efficiency does not change so much even if $B_{res}(= 2\pi f m/q)$ deviates from B_{axis}. But the transferred power to majority ions and electrons decreases at the center region. In the finite β case the heating efficiencies are reduced if the position of the resonance layer is moved from the layer with $B_{res} = B_{axis}$. The maximum heating efficiency can be obtained when the frequency is adjusted to the magnetic field strength at the axis.

The inclusion of the finite $k_{\parallel}$ does not change the heating efficiency so much and the small degradation of the heating efficiency is found in the large $k_{\parallel}$ case. However the small increase of the heating efficiency (~ 10%)

can be seen when the multiple $k_{\|}$ waves are applied.

3. SELF-DETERMINED RADIAL ELECTRIC FIELD

Since energetic minority ions due to interactions with RF-fields have a large gyroradius and drift velocity, their particle flux across the flux surface has significant effects on the radial electric field, which is determined by the ambipolar condition. Here, the equation determining the radial electric field in the presence of the fast ions (energetic minority ions in the present case) is proposed. The main assumptions for the background thermal species are 1) the standard small gyroradius ordering, 2) the transport ordering, 3) the drift ordering, 4) no inductive electric field, and 5) the fast time variation of the radial electric field in comparison to the background density and pressure.

Finally, we treat effects of the fast ions on the thermal species as the external forces. Since the behavior of the fast ions is calculated by the Monte-Carlo simulation, the effects of the fast ions enter the final equation as the radial flux and the Coulomb interaction (friction) with the background thermal species in terms of the external force. Note that the inductive electric field is neglected. As a result of it, we have the following equation in the Boozer coordinate system (ψ, θ, ζ):

$$\varepsilon_0(1+\varepsilon_{rr})\left\langle|\nabla\psi|^2\right\rangle\frac{\partial}{\partial t}\left(\frac{d\Phi(\psi)}{d\psi}\right)=e_f\Gamma_f^{\psi}+\sum_a e_a\Gamma_a^{\psi}+\sum_a R_{af} \tag{1}$$

where the summation is taken only for the thermal species, and Γ_f^{ψ} is the radial flux of the fast ions and Γ_a^{ψ} is the radial fluxes of the thermal species a due to the $1/\nu$ ripple diffusion. Note that Γ_f^{ψ} $(=\langle n_f\vec{u}_f\cdot\nabla\psi\rangle)$ includes the fast ion particle loss. The residual term $\sum_a R_{af}$ is the Coulomb frictional flux of the fast ions with thermal species and is neglected in this calculation.

Other quantities are defined as follows:

$$\varepsilon_{rr} = \left[\left\langle\frac{|\nabla\psi|^2}{v_A^2}\right\rangle+\frac{\left\langle g_2\left(J\frac{\partial G}{\partial\theta}-I\frac{\partial G}{\partial\zeta}\right)\right\rangle}{\left\langle v_A^2\right\rangle}\right]\times\frac{c^2}{\left\langle|\nabla\psi|^2\right\rangle} \tag{2}$$

$$v_A^2 = \frac{B^2}{\sum_a m_a n_a \mu_0} \tag{3}$$

The functions G and g_2 are given as the solutions of the following equations:

$$\begin{aligned}\vec{B}\cdot\nabla G &= \frac{1}{\sqrt{g}}\left\{\frac{\left\langle B^2\right\rangle}{B^2}-1\right\}\\ \vec{B}\cdot\nabla\left(\frac{g_2}{B^2}\right) &= \vec{B}\times\nabla\psi\cdot\nabla\left(\frac{1}{B^2}\right)\end{aligned} \tag{4}$$

Both are determined only by the magnetic field configuration.

We study the ICRF minority heating for the LHD including the self-consistent radial electric field. We use Eq. (1) for the time development of the radial electric field E_ψ. We calculate the radial particle fluxes for electrons and majority ions, Γ_e^ψ and Γ_i^ψ, respectively, using the neoclassical diffusion theory. The radial flux for energetic minority ions Γ_f^ψ is calculate by the present Monte Carlo simulation code MOMOCO. Figure 3 shows the time development of the radial electric field during the ICRF heating. The calculation parameters are the same as in Fig. 2. We find an enhancement of the strong negative radial electric field at the periphery due to the radial flux of escaping energetic minority ions out of the last closed surface and E_ψ is larger for higher β plasma because of the large loss region of high energetic ions. Moreover, it should be noted that the neoclassical ion flux can become inward at the plasma periphery as the radial electric field increases as seen in Fig. 4.

Thus the possibility has been shown that the large electric field enhanced by loss of energetic ions can control the plasma transport. To investigate the influence of energetic ions on the profile of majority ions and electrons, the simulation is carried out incorporating a transport code with the present Monte Carlo code.

ACKNOWLEDGEMENTS

The authors wish to thank Dr. A. Fukuyama, Dr. K. Ichiguchi and K. Nishimura for useful discussions. They also thank Prof. A. Iiyoshi and Prof. T. Sato for continuous encouragement. The calculations were carried out on the super computer SX-3 at the National Institute for Fusion Science.

REFERENCES

[1] MUTOH, T., et al., Nucl. Fusion **24** (1984) 1003.

[2] MUTOH, T., et al., in Plasma Physics Controlled Nuclear Fusion Research 1986 (Proc. 11th Int. Conf. Kyoto, 1986), Vol. 2, IAEA, Vienna (1987) 473.

[3] KWON, M., et al., Nucl. Fusion **32** (1992) 1225.

[4] OKAMURA, S., et al., in Plasma Physics Controlled Nuclear Fusion Research 1992 (Proc. 14th Int. Conf. Würzburg, 1992), Vol. 2, IAEA, Vienna (1992) 507.

[5] IIYOSHI, A., et al., Fusion Technol. **17** (1990) 148.

[6] MURAKAMI, S., et al., to be published in Nucl. Fusion **34** (1944).

[7] MURAKAMI, S., et al., to be published in Fusion Eng. Design.

[8] HIRSHMAN, S.P., WHITSON, J.C., Phys. Fluids **26** (1983) 3553.

[9] ITOH, K., et al., Nucl. Fusion **29** (1989) 1851.

[10] ITOH, K., et al., Phys. Fluids B **3** (1991) 1294.

FIGURE CAPTIONS

FIG. 1. Typical orbits of minority ions in the ICRF heating for two different plasma β configurations: (a) $\beta = 0\%$, (b) $\beta = 6.0\%$.

FIG. 2. Heating efficiencies as a function of the absorption power changing the plasma β and minority species (H and ^3He).

FIG. 3. Build up of the radial electric field including the flux of energetic minority ions ($\beta = 0.0$ and 6.0%).

FIG. 4. Radial particle fluxes for electrons and majority ions. The inward ion flux can be seen at the plasma periphery.

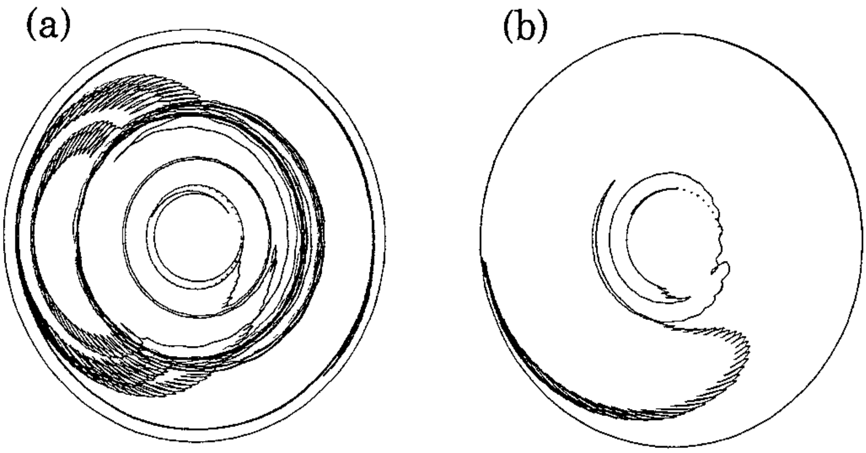
(a)
(b)

Fig. 1

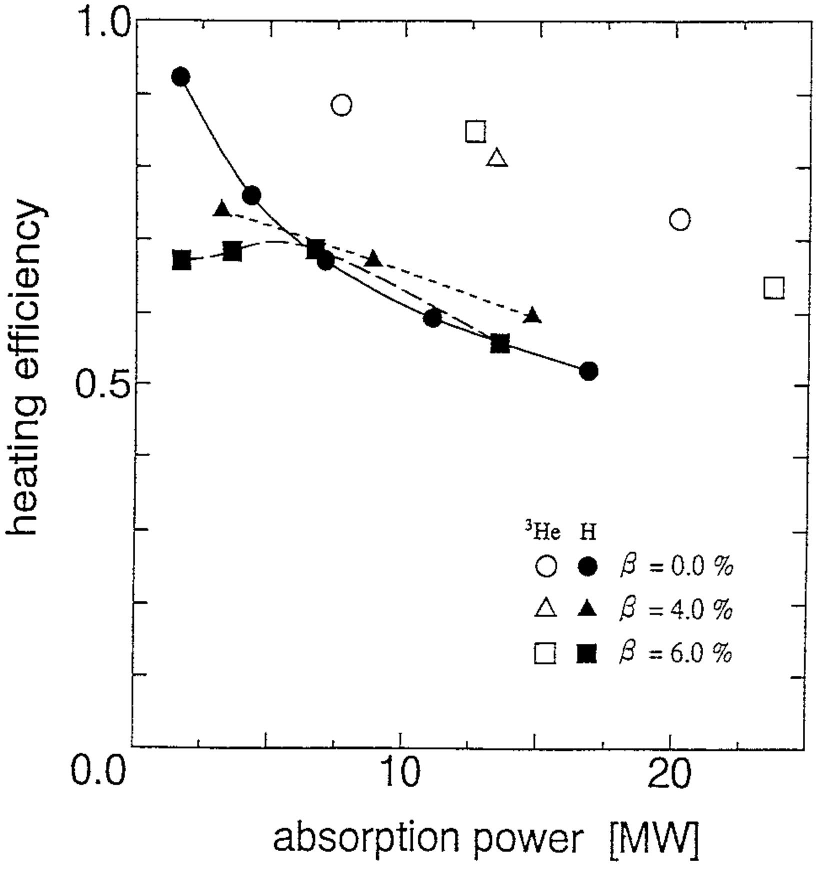
1.0
0.5
0.0
10
20
heating efficiency
absorption power [MW]
3He H
β = 0.0 %
β = 4.0 %
β = 6.0 %

Fig. 2

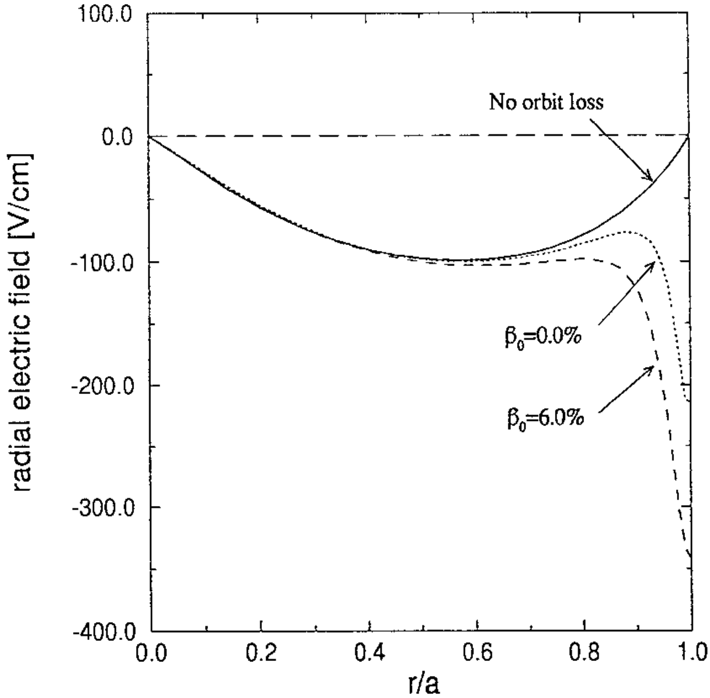
100.0
0.0
-100.0
-200.0
-300.0
-400.0
radial electric field [V/cm]
No orbit loss
β_0=0.0%
β_0=6.0%
0.0
0.2
0.4
0.6
0.8
1.0
r/a

Fig. 3

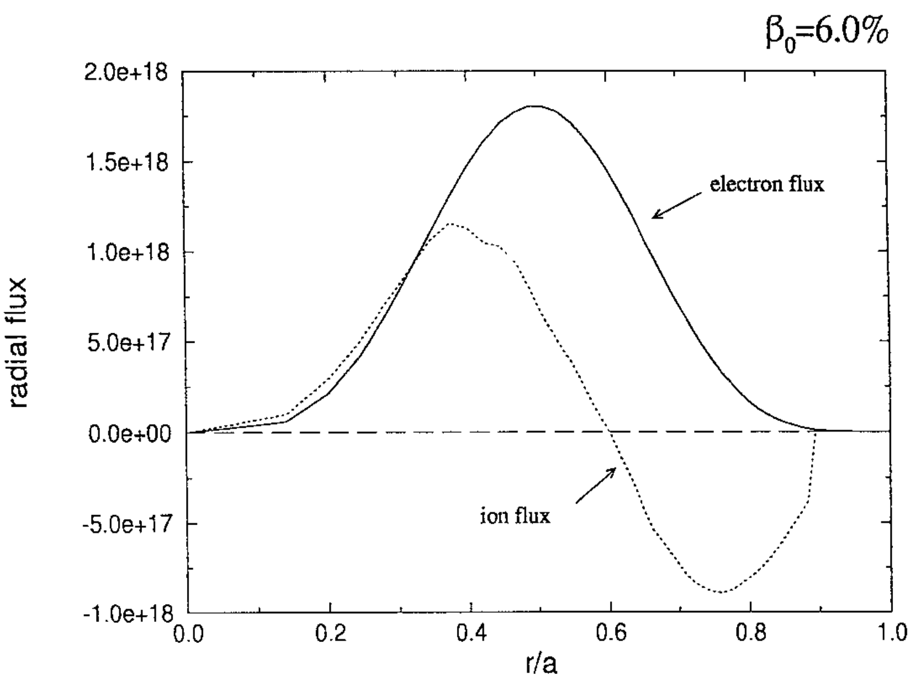
β_0=6.0%
2.0e+18
1.5e+18
1.0e+18
5.0e+17
0.0e+00
-5.0e+17
-1.0e+18
radial flux
electron flux
ion flux
0.0
0.2
0.4
0.6
0.8
1.0
r/a

Fig. 4

Recent Issues of NIFS Series

NIFS-268 T. Shikama, C. Namba, M. Kosuda, Y. Maeda,
Development of High Time-Resolution Laser Flash Equipment for Thermal Diffusivity Measurements Usting Miniature-Size Specimens; Jan. 1994

NIFS-269 T. Hayashi, T. Sato, P. Merkel, J. Nührenberg, U. Schwenn,
Formation and 'Self-Healing' of Magnetic Islands in Finite-β Helias Equilibria; Jan. 1994

NIFS-270 S. Murakami, M. Okamoto, N. Nakajima, T. Mutoh,
Efficiencies of the ICRF Minority Heating in the CHS and LHD Plasmas; Jan. 1994

NIFS-271 Y. Nejoh, H. Sanuki,
Large Amplitude Langmuir and Ion-Acoustic Waves in a Relativistic Two-Fluid Plasma; Feb. 1994

NIFS-272 A. Fujisawa, H. Iguchi, A. Taniike, M. Sasao, Y. Hamada,
A 6MeV Heavy Ion Beam Probe for the Large Helical Device; Feb. 1994

NIFS-273 Y. Hamada, A. Nishizawa, Y. Kawasumi, K. Narihara, K. Sato, T. Seki, K. Toi, H. Iguchi, A. Fujisawa, K. Adachi, A. Ejiri, S. Hidekuma, S. Hirokura, K. Ida, J. Koong, K. Kawahata, M. Kojima, R. Kumazawa, H. Kuramoto, R. Liang, H. Sakakita, M. Sasao, K. N. Sato, T. Tsuzuki, J. Xu, I. Yamada, T. Watari, I. Negi,
Measurement of Profiles of the Space Potential in JIPP T-IIU Tokamak Plasmas by Slow Poloidal and Fast Toroidal Sweeps of a Heavy Ion Beam; Feb. 1994

NIFS-274 M. Tanaka,
A Mechanism of Collisionless Magnetic Reconnection; Mar. 1994

NIFS-275 A. Fukuyama, K. Itoh, S.-I. Itoh, M. Yagi and M. Azumi,
Isotope Effect on Confinement in DT Plasmas; Mar. 1994

NIFS-276 R.V. Reddy, K. Watanabe, T. Sato and T.H. Watanabe,
Impulsive Alfven Coupling between the Magnetosphere and Ionosphere; Apr.1994

NIFS-277 J. Uramoto,
A Possibility of π^- Meson Production by a Low Energy Electron Bunch and Positive Ion Bunch; Apr. 1994

NIFS-278 K. Itoh, S.-I. Itoh, A. Fukuyama, M. Yagi and M. Azumi,
Self-sustained Turbulence and L-mode Confinement in Toroidal Plasmas

II; Apr. 1994

NIFS-279 K. Yamazaki and K.Y.Watanabe,
New Modular Heliotron System Compatible with Closed Helical Divertor and Good Plasma Confinement; Apr. 1994

NIFS-280 S. Okamura, K. Matsuoka, K. Nishimura, K. Tsumori, R. Akiyama, S. Sakakibara, H. Yamada, S. Morita, T. Morisaki,. N. Nakajima, K. Tanaka, J. Xu, K. Ida, H. Iguchi, A. Lazaros, T. Ozaki, H. Arimoto, A. Ejiri, M. Fujiwara, H. Idei. O. Kaneko, K. Kawahata, T. Kawamoto, A. Komori, S. Kubo, O. Motojima, V.D. Pustovitov, C. Takahashi, K. Toi and I. Yamada,
High-Beta Discharges with Neutral Beam Injection in CHS; Apr. 1994

NIFS-281 K. Kamada, H. Kinoshita and H. Takahashi,
Anomalous Heat Evolution of Deuteron Implanted Al on Electron Bombardment ; May 1994

NIFS-282 H. Takamaru, T. Sato, K. Watanabe and R. Horiuchi,
Super Ion Acoustic Double Layer; May 1994

NIFS-283 O.Mitarai and S. Sudo
Ignition Characteristics in D-T Helical Reactors; June 1994

NIFS-284 R. Horiuchi and T. Sato,
Particle Simulation Study of Driven Magnetic Reconnection in a Collisionless Plasma; June 1994

NIFS-285 K.Y. Watanabe, N. Nakajima, M. Okamoto, K. Yamazaki, Y. Nakamura, M. Wakatani,
Effect of Collisionality and Radial Electric Field on Bootstrap Current in LHD (Large Helical Device); June 1994

NIFS-286 H. Sanuki, K. Itoh, J. Todoroki, K. Ida, H. Idei, H. Iguchi and H. Yamada,
Theoretical and Experimental Studies on Electric Field and Confinement in Helical Systems; June 1994

NIFS-287 K. Itoh and S-I. Itoh,
Influence of the Wall Material on the H-mode Performance; June 1994

NIFS-288 K. Itoh, A. Fukuyama, S.-I. Itoh, M. Yagi and M. Azumi
Self-Sustained Magnetic Braiding in Toroidal Plasmas: July 1994

NIFS-289 Y. Nejoh,
Relativistic Effects on Large Amplitude Nonlinear Langmuir Waves in a Two-Fluid Plasma; July 1994

NIFS-290 N. Ohyabu, A. Komori, K. Akaishi, N. Inoue, Y. Kubota, A.I. Livshit,

N. Noda, A. Sagara, H. Suzuki, T. Watanabe, O. Motojima, M. Fujiwara, A. Iiyoshi,
Innovative Divertor Concepts for LHD; July 1994

NIFS-291 H. Idei, K. Ida, H. Sanuki, S. Kubo, H. Yamada, H. Iguchi, S. Morita, S. Okamura, R. Akiyama, H. Arimoto, K. Matsuoka, K. Nishimura, K. Ohkubo, C. Takahashi, Y. Takita, K. Toi, K. Tsumori and I. Yamada,
Formation of Positive Radial Electric Field by Electron Cyclotron Heating in Compact Helical System; July 1994

NIFS-292 N. Noda, A. Sagara, H. Yamada, Y. Kubota, N. Inoue, K. Akaishi, O. Motojima, K. Iwamoto, M. Hashiba, I. Fujita, T. Hino, T. Yamashina, K. Okazaki, J. Rice, M. Yamage, H. Toyoda and H. Sugai,
Boronization Study for Application to Large Helical Device; July 1994

NIFS-293 Y. Ueda, T. Tanabe, V. Philipps, L. Könen, A. Pospieszczyk, U. Samm, B. Schweer, B. Unterberg, M. Wada, N. Hawkes and N. Noda,
Effects of Impurities Released from High Z Test Limiter on Plasma Performance in TEXTOR; July. 1994

NIFS-294 K. Akaishi, Y. Kubota, K. Ezaki and O. Motojima,
Experimental Study on Scaling Law of Outgassing Rate with A Pumping Parameter, Aug. 1994

NIFS-295 S. Bazdenkov, T. Sato, R. Horiuchi, K. Watanabe
Magnetic Mirror Effect as a Trigger of Collisionless Magnetic Reconnection, Aug. 1994

NIFS-296 K. Itoh, M. Yagi, S.-I. Itoh, A. Fukuyama, H. Sanuki, M. Azumi
Anomalous Transport Theory for Toroidal Helical Plasmas, Aug. 1994 (IAEA-CN-60/D-III-3)

NIFS-297 J. Yamamoto, O. Motojima, T. Mito, K. Takahata, N. Yanagi, S. Yamada, H. Chikaraishi, S. Imagawa, A. Iwamoto, H. Kaneko, A. Nishimura, S. Satoh, T. Satow, H. Tamura, S. Yamaguchi, K. Yamazaki, M. Fujiwara, A. Iiyoshi and LHD group,
New Evaluation Method of Superconductor Characteristics for Realizing the Large Helical Device; Aug. 1994 (IAEA-CN-60/F-P-3)

NIFS-298 A. Komori, N. Ohyabu, T. Watanabe, H. Suzuki, A. Sagara, N. Noda, K. Akaishi, N. Inoue, Y. Kubota, O Motojima, M. Fujiwara and A. Iiyoshi,
Local Island Divertor Concept for LHD; Aug. 1994 (IAEA-CN-60/F-P-4)

NIFS-299 K. Toi, T. Morisaki, S. Sakakibara, A. Ejiri, H. Yamada, S. Morita, K. Tanaka, N. Nakjima, S. Okamura, H. Iguchi, K. Ida, K. Tsumori, S. Ohdachi, K. Nishimura, K. Matsuoka, J. Xu, I. Yamada, T. Minami, K. Narihara, R. Akiyama, A. Ando, H. Arimoto, A. Fujisawa, M. Fujiwara, H. Idei, O. Kaneko, K. Kawahata, A. Komori, S. Kubo, R. Kumazawa, T. Ozaki, A. Sagara, C. Takahashi, Y. Takita and T. Watari

Impact of Rotational-Transform Profile Control on Plasma Confinement and Stability in CHS; Aug. 1994 (IAEA-CN-60/A6/C-P-3)

NIFS-300 H. Sugama and W. Horton,
Dynamical Model of Pressure-Gradient-Driven Turbulence and Shear Flow Generation in L-H Transition; Aug. 1994 (IAEA/CN-60/D-P-I-11)

NIFS-301 Y. Hamada, A. Nishizawa, Y. Kawasumi, K.N. Sato, H. Sakakita, R. Liang, K. Kawahata, A. Ejiri, K. Narihara, K. Sato, T. Seki, K. Toi, K. Itoh, H. Iguchi, A. Fujisawa, K. Adachi, S. Hidekuma, S. Hirokura, K. Ida, M. Kojima, J. Koog, R. Kumazawa, H. Kuramoto, T. Minami, I. Negi, S. Ohdachi, M. Sasao, T. Tsuzuki, J. Xu, I. Yamada, T. Watari,
Study of Turbulence and Plasma Potential in JIPP T-IIU Tokamak; Aug. 1994 (IAEA/CN-60/A-2-III-5)

NIFS-302 K. Nishimura, R. Kumazawa, T. Mutoh, T. Watari, T. Seki, A. Ando, S. Masuda, F. Shinpo, S. Murakami, S. Okamura, H. Yamada, K. Matsuoka, S. Morita, T. Ozaki, K. Ida, H. Iguchi, I. Yamada, A. Ejiri, H. Idei, S. Muto, K. Tanaka, J. Xu, R. Akiyama, H. Arimoto, M. Isobe, M. Iwase, O. Kaneko, S. Kubo, T. Kawamoto, A. Lazaros, T. Morisaki, S. Sakakibara, Y. Takita, C. Takahashi and K. Tsumori,
ICRF Heating in CHS; Sep. 1994 (IAEA-CN-60/A-6-I-4)

NIFS-303 S. Okamura, K. Matsuoka, K. Nishimura, K. Tsumori, R. Akiyama, S. Sakakibara, H. Yamada, S. Morita, T. Morisaki, N. Nakajima, K. Tanaka, J. Xu, K. Ida, H. Iguchi, A. Lazaros, T. Ozaki, H. Arimoto, A. Ejiri, M. Fujiwara, H. Idei, A. Iiyoshi, O, Kaneko, K. Kawahata, T. Kawamoto, S. Kubo, T. Kuroda, O. Motojima, V.D. Pustovitov, A. Sagara, C. Takahashi, K. Toi and I. Yamada,
High Beta Experiments in CHS; Sep. 1994 (IAEA-CN-60/A-2-IV-3)

NIFS-304 K. Ida, H. Idei, H. Sanuki, K. Itoh, J. Xu, S. Hidekuma, K. Kondo, A. Sahara, H. Zushi, S.-I. Itoh, A. Fukuyama, K. Adati, R. Akiyama, S. Bessho, A. Ejiri, A. Fujisawa, M. Fujiwara, Y. Hamada, S. Hirokura, H. Iguchi, O. Kaneko, K. Kawahata, Y. Kawasumi, M. Kojima, S. Kubo, H. Kuramoto, A. Lazaros, R. Liang, K. Matsuoka, T. Minami, T. Mizuuchi, T. Morisaki, S. Morita, K. Nagasaki, K. Narihara, K. Nishimura, A. Nishizawa, T. Obiki, H. Okada, S. Okamura, T. Ozaki, S. Sakakibara, H. Sakakita, A. Sagara, F. Sano, M. Sasao, K. Sato, K.N. Sato, T. Saeki, S. Sudo, C. Takahashi, K. Takaka, K. Tsumori, H.Yamada, I. Yamada, Y. Takita, T. Tuzuki, K. Toi and T. Watari,
Control of Radial Electric Field in Torus Plasma; Sep. 1994 (IAEA-CN-60/A-2-IV-2)

NIFS-305 T. Hayashi, T. Sato, N. Nakajima, K. Ichiguchi, P. Merkel, J. Nührenberg, U. Schwenn, H. Gardner, A. Bhattacharjee and C.C.Hegna,
Behavior of Magnetic Islands in 3D MHD Equilibria of Helical Devices; Sep. 1994 (IAEA-CN-60/D-2-II-4)